



Arctic Sea Ice Melt Pond Statistics and Maps, 1999-2001, Version 1

USER GUIDE

How to Cite These Data

As a condition of using these data, you must include a citation:

Fetterer, F., S. Wilds, and J. Sloan. 2008. *Arctic Sea Ice Melt Pond Statistics and Maps, 1999-2001, Version 1*. [Indicate subset used]. Boulder, Colorado USA. NSIDC: National Snow and Ice Data Center. <https://doi.org/10.7265/N5PK0D32>. [Date Accessed].

FOR QUESTIONS ABOUT THESE DATA, CONTACT NSIDC@NSIDC.ORG

FOR CURRENT INFORMATION, VISIT <https://nsidc.org/data/G02159>



National Snow and Ice Data Center

TABLE OF CONTENTS

1	OVERVIEW	2
1.1	Background and Data Set Applications	2
1.2	Project History	3
1.3	Site Selection.....	3
1.4	Observations Concerning the Melt Season and its Variability	6
2	DETAILED DATA DESCRIPTION.....	10
2.1	Product Formats	10
2.1.1	Image Files	11
2.1.2	Data Files for Surface Type Coverage Statistics	13
2.1.3	Data Files for Pond Size Statistics	14
2.1.4	Data File Summary Information	15
3	DATA ACQUISITION AND PROCESSING.....	19
3.1	Summary	19
3.2	Data Processing	20
3.3	Quality Assessment.....	21
4	REFERENCES AND RELATED PUBLICATIONS	22
4.1	Related Data Collections.....	24
4.2	Related Websites	24
5	CONTACTS AND ACKNOWLEDGMENTS	24
6	DOCUMENT INFORMATION.....	25
6.1	Document Authors.....	25
6.2	Publication Date	25
6.3	Date Last Updated.....	25

1 OVERVIEW

Visible band imagery from high-resolution satellites were acquired over four Arctic Ocean sites (three in 1999) during the summers of 1999, 2000, and 2001. The sites were within the median extent of the perennial ice pack. Imagery was analyzed using supervised maximum likelihood classification to derive either two (water and ice) or three (pond, open water, and ice) surface classes. Clouds were masked by hand. The data set consists of tables of pond coverage and size statistics for 500 m square cells within 10 km square images (image resolution is 1 meter), along with the surface type maps called Image Derived Products (IDPs) from which the pond statistics were derived. A total of 101 images over the three summers and four sites were used for pond statistics, out of a total of 1056 images acquired. The images are irregularly spaced in time.

Data are stored in Microsoft Excel format and ASCII text, image files are stored as GeoTIFF binary images, browse images in PNG, and JPG image files, and are available from August 1999 and generally for May into September for 2000 and 2001 via FTP.

1.1 Background and Data Set Applications

The surface energy balance of arctic sea ice in summer is largely determined by ice surface characteristics. The extent of melt ponding is the most important of these characteristics because the albedo of a melt pond is about 30 percent lower than that of the surrounding ice. As a result, changes in ice floe albedo are linearly related to changes in floe pond coverage. The sea ice-albedo feedback mechanism dictates that a reduction in ice albedo due to an increase in pond coverage leads to greater absorption of solar radiation, increased melting, and further reduction in albedo through the summer melt season. Sea ice mass balance is sensitive to the shortwave radiation balance in summer. Ice albedo determines net absorbed solar radiation and must therefore be accurately specified in models that attempt to simulate the seasonal cycle of sea ice.

These data provide information on the timing and extent of melt pond formation, information that is needed to fully understand the impact of ponds on ice thermodynamics and to improve parameterizations of albedo in models. Relatively little pond coverage data exists. Readily available satellite data do not resolve ponds, and the cloudy arctic summer makes airborne surveys difficult. The Surface Heat Balance of the Arctic Ocean (SHEBA) experiment was designed in part to provide needed melt pond and ancillary data. The data set provided here helps researchers to place these and other observations in an arctic-wide context, addressing the need for a multiyear time series from widely-spaced regions. Applications include using it to characterize surface conditions and their impact on the net radiation balance; to study pond development in response to changes in temperature, cloud cover, and insolation; and to aid in parameterizing ice albedo for inclusion in climate models.

1.2 Project History

Development of this data set was based on experience gained using reconnaissance imagery during SHEBA and earlier summer ice monitoring experiments (NSIDC 2000, Fetterer and Untersteiner 1998a). In 1999, Imagery Derived Products (unclassified versions of imagery) were created from 57 high-resolution images of the SHEBA experiment site. The images were initially made available through the NSF Arctic System Science (ARCSS) Data Coordination Center at NSIDC, and in 2008 were transferred to the NOAA program at NSIDC. See the [SHEBA Reconnaissance Imagery](#) data set. The optical band images cover a variable area on the order of 15 kilometers by 40 kilometers at an average resolution of slightly over 1 meter. This data set is based on similar imagery. In this case, however, only the surface type maps, and not the original imagery itself, have been released. Another difference is that SHEBA and earlier reconnaissance image acquisitions attempted to follow the same ice over time in a Lagrangian trajectory. Here, the objective was a better spatial and temporal sample of imagery than could be obtained by the manually intensive method of tracking ice floes as they drifted over time. Work was done in partnership with the Rex (Rapid Exploitation) National Civil Applications Program (NCAP) at the USGS Rocky Mountain Geographic Science Center (RMGSC, formerly the Rocky Mountain Mapping Center), Lakewood, CO, and with the USGS Advanced Systems Center (ASC), Reston, VA. ASC acquired the data. RMGSC has facilities for working with classified data from high-resolution satellites. There, coverage statistics and surface type map (Image Derived Products or IDPs), were created under the direction of the PI using supervised maximum likelihood classification.

1.3 Site Selection

Four sites were selected to cover disparate regions of the Arctic Ocean. The sites were abbreviated as Beaufo for the Beaufort Sea, Cacana for the Canadian Arctic, Cafram for the Fram Strait, and Esiber for the East Siberian Sea. Refer to Figure 1..

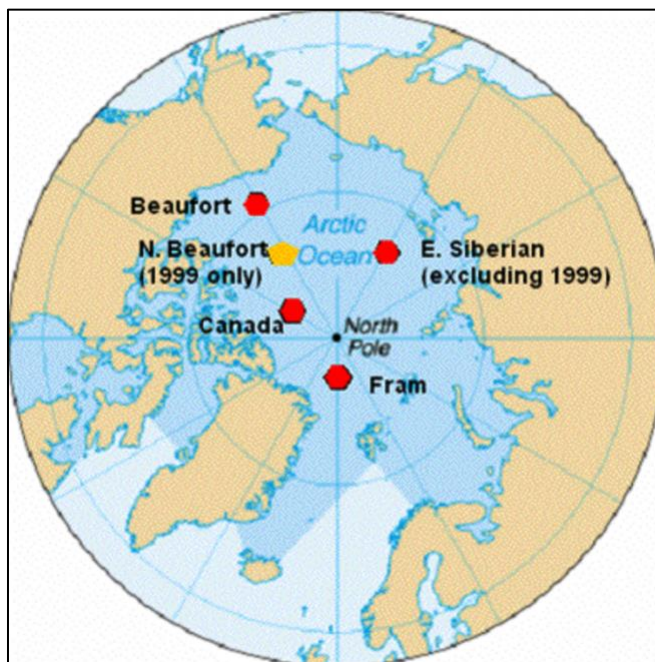


Figure 1. Site map for imagery collection. The area at each site over which imagery was acquired was about 2 degrees in longitude and 0.25 degrees in latitude. The site labeled N. Beaufort was mistakenly acquired in 1999 only, and the E. Siberian site was omitted that year. The N. Beaufort images were not processed for pond statistics. [Click for larger image.](#)

Table 1 supplies the abbreviated site names, locations upon which data acquisition was centered, and years over which imagery was collected in the summer months, generally mid-May to mid-September.

Table 1. Site Names, Locations, and Years of Imagery Collected from Mid-May to Mid-September

Site Name	Latitude	Longitude	Years
Beaupo	73° N	150° W	1999, 2000, 2001
Cacana	85° N	120° W	1999, 2000, 2001
Cafram	85° N	0° E	1999, 2000, 2001
Esiber	82° N	150° E	2000, 2001

The relation of these sites to the ice edge and the median ice extent at the end of summer in each year is illustrated by Figure 2. Similar figures for May through September are available in the ancillary data directory

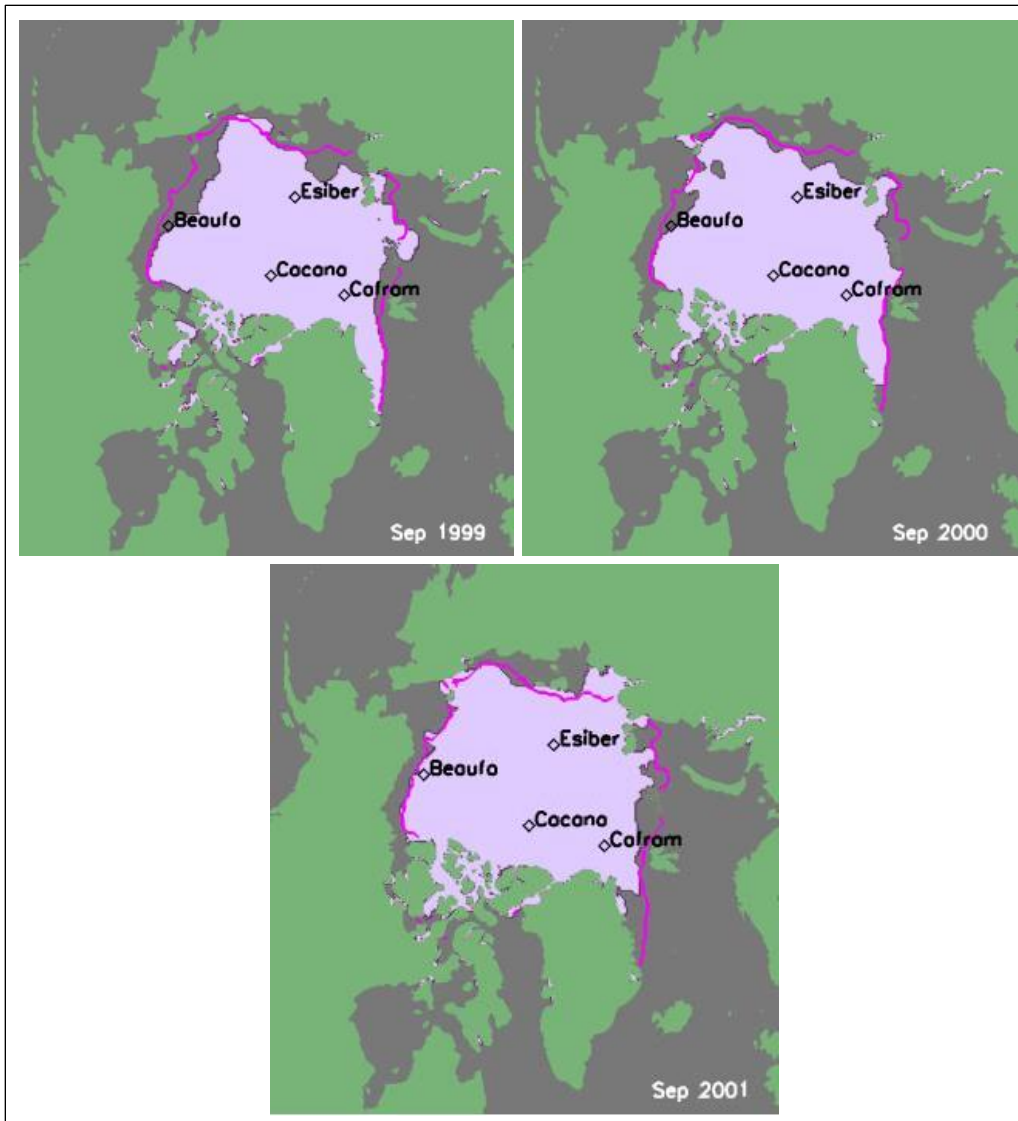


Figure 2. Site locations relative to the median (1979 to 2000) September ice edge position (pink line) and the September ice extent in 1999, 2000, and 2001. The ice extent and median position of the edge are from the [Sea Ice Index](#), and are derived from passive microwave imagery. Similar maps are available for all three years and for each summer month beginning in May

The sites are all within the perennial pack although the Beaufort site is at its edge. Most of the ice sampled can be assumed to be multiyear ice, although ice having the appearance of first-year (smoother, with heavier pond coverage in most cases) is present. The IDPs showed characteristic differences in the texture of pond coverage on smooth and deformed ice. Ponds on thin or undeformed ice often appeared in a regular linear pattern. This ice had much higher melt pond coverage (30 percent to 50 percent) than that of the more prevalent adjacent deformed ice (15 percent to 25 percent).

1.4 Observations Concerning the Melt Season and its Variability

The following observations concerning the progression of the melt season and its variability were made in the course of working with the imagery. A detailed analysis was not completed.

The images are irregularly spaced in time, and often separated by a week or more, so the record of pond evolution has gaps. However, major events were usually discernible: darkening of snow; the appearance of the first few small, round ponds, followed by ice that appeared almost flooded with high pond coverage; then some reduction in coverage and the appearance of channels (channels were not always present); and finally the formation of new ice in leads (except at the Beaufort site, which was near the ice edge). In some years and for some sites, many ponds appeared to freeze over, but remained distinct as ponds, for a week or more (Cacana, in 1999, is an example). Ponds often appeared to freeze over well before the first appearance of ice in leads (Esiber, in 2000, is an example).

The onset of melt was not always clearly detectable. One image might show what appeared to be darkened snow or a few small ponds, while the next in the sequence had no such signs of melt onset. This could be because the images did not capture the same ice, or because new snow had fallen. Similarly, freeze-up did not always follow a predictable course. New ice could be forming in leads, while at the same time ponds remained distinct for several more weeks (Cafram, in 2001, is an example).

Figures 3a – 3d from the Cacana site are one example of the evolution described above. From the first appearance of widespread ponds (June 22, 13 percent average for cell pond coverage, with 5 percent standard deviation) with rapid evolution to a nearly flooded state (June 28, 31 percent coverage, 10 percent standard deviation), followed by a slow reduction in pond coverage (July 5, 19 percent coverage, 4 percent standard deviation, and August 15, 16 percent coverage, 4 percent standard deviation). Figures 4a – 4c from the Beaufort site provide a different example. Here pond coverage evolved from 26 percent on June 28 to 18 percent on July 16, but then rose again to 32 percent on September 3. The location of this site near the ice edge was a factor, as ice melted away rather than refroze at summer's end. Pond coverage statistics are the average and standard deviation for all cells containing less than 5 percent open water. Table 2 shows the date melt events were observed in the imagery.

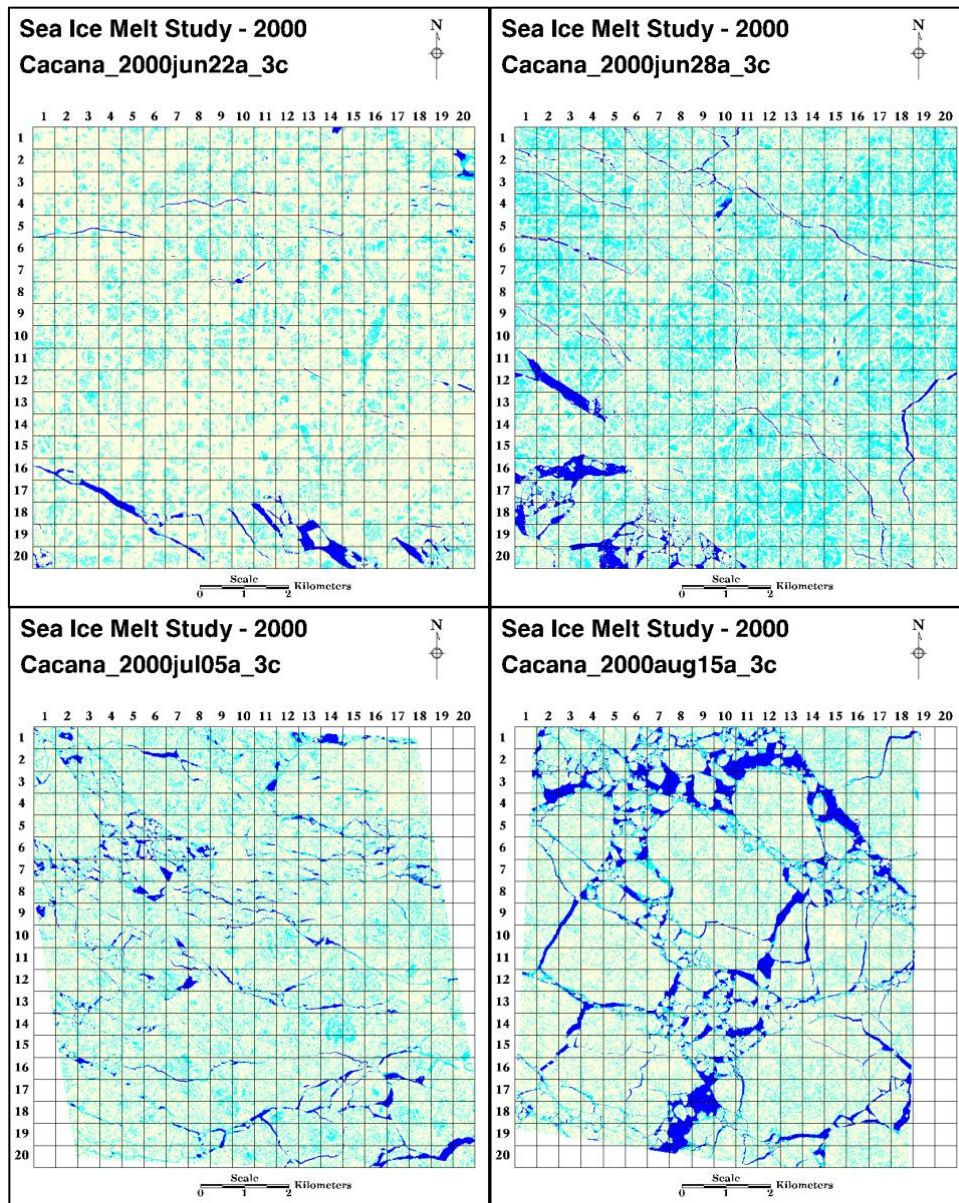


Figure 3a-3d. A selection of surface type map browse images showing the evolution of ice at the Cacana site in 2000. These are three class products. Cyan is pond, blue is open water, and white is ice.

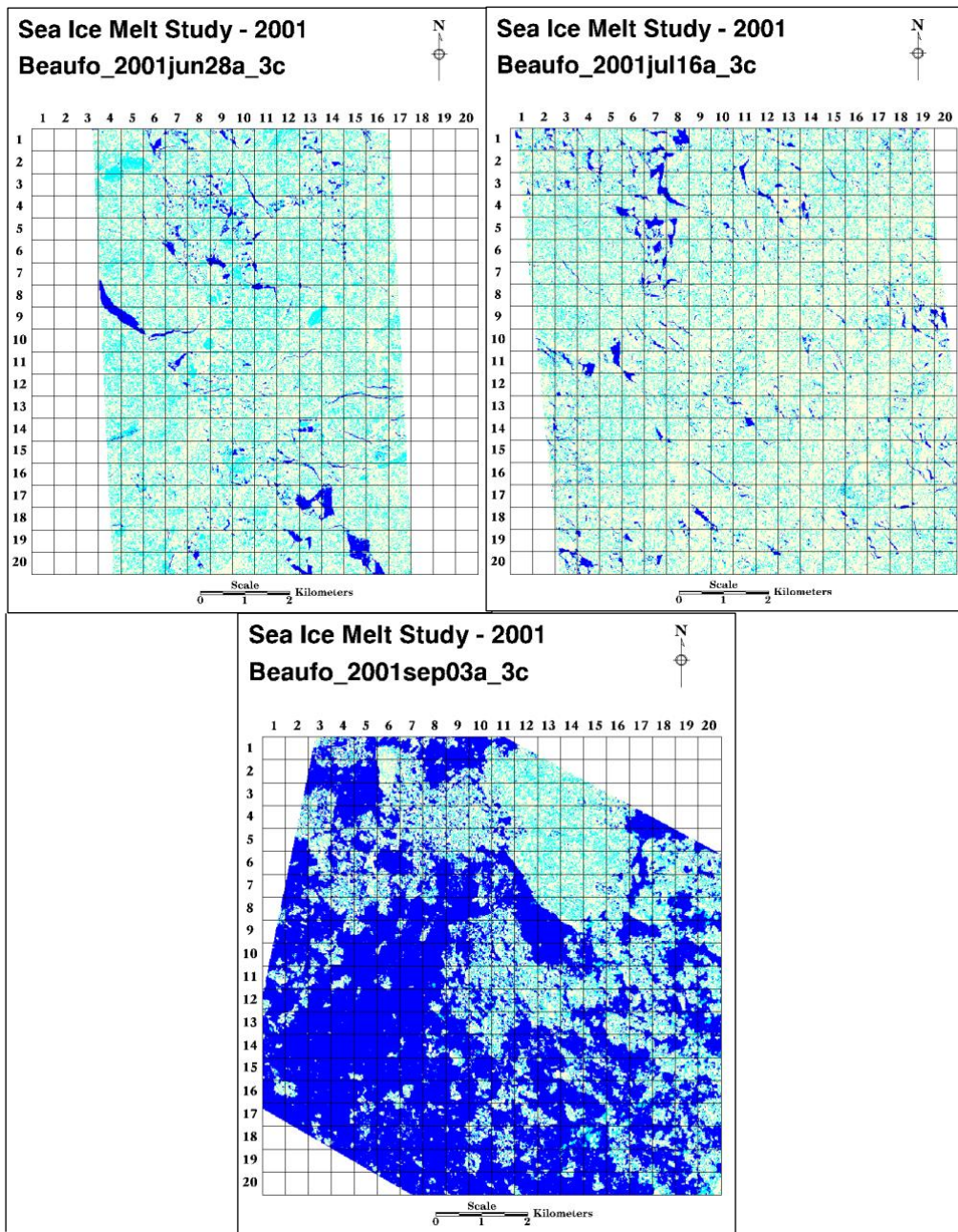


Figure 4a-4c. A selection of surface type map browse images showing the evolution of ice at the Beaufort site in 2001.

Note: In Table 2, the dates are the dates that the indicated event took place, and not necessarily the date on which it takes place, due to gaps in the image sequence.

Table 2. An Overview of Melt Season Evolution for Each Site

Site	Date	First Image Reviewed	Dark Snow	First Ponds	Flooded	First New Ice in Leads	Last Image Reviewed	Notes
Beaufort	1999	27-Jun	Unknown	Unknown	Unknown	Unknown	15-Sep	Melt was in progress at first image. Ice appears rotten, nearly submerged in 28 June image.
	2000	8-May	8-May	Unknown	21-Jun	Unknown	3-Sep	Rotten ice by 15 August. Season ended with rotten ice and open water.
	2001	18-May	30-May	13-Jun	21-Jun	Unknown	3-Sep	30 May image quality is bad, dark snow may be false impression.
Cacana	1999	7-Jul	Unknown	Unknown	Unknown	17-Aug	27-Aug	Melt was in progress at first image. Ponds appeared to be beginning to drain, with some channels.
	2000	5-May	16-May	Unknown	22-Jun	15-Aug	2-Sep	
	2001	16-May	3-Jun	24-Jun	Unknown	22-Aug	9-Sep	

Site	Date	First Image Reviewed	Dark Snow	First Ponds	Flooded	First New Ice in Leads	Last Image Reviewed	Notes
Cafram	1999	26-Jun	Unknown	Unknown	26-Jun	21-Aug	12-Sep	Melt was in progress at first image, with the distinctive appearance of flooded ice.
	2000	3-May	21-Jun	Unknown	27-Jun	4-Sep	4-Sep	
	2001	25-May	24-Jun	24-Jun	13-Jul	5-Aug	2-Sep	Some new ice on 4 Aug, and still distinct ponds on 2 Sep.
Esiber	1999	N/A	N/A	N/A	N/A	N/A	N/A	
	2000	7-May	26-May	1-Jun	4-Jul	1-Sep	1-Sep	
	2001	17-May	20-Jun	1-Jul	Unknown	27-Aug	12-Sep	

2 DETAILED DATA DESCRIPTION

2.1 Product Formats

Table 3 summarizes the number of images per site per summer from which products were created. An additional 11 images of quality 4 (poor) were not used for pond statistics, but were retained as PNG browse files because they give an indication of floe morphology. A total of 101 images were used for data products. This number fell short of the anticipated 30 images per site per summer, although a much larger number was initially selected as potentially usable (except in 1999, when relatively few images were acquired by ASC). Reliable supervised classification results proved difficult to obtain for many images. Ridge shadows were a particularly difficult problem at the most northerly sites, Cacana and Cafram, where the short season reduced the number of images available, and the short time span during which ice was properly illuminated for good classification, combined with low sun angle, compromised good pond coverage statistics for all but a few images.

See Table 4 for a complete list of data products and file naming conventions.

Note: In Table 3, the values for Quality are: 1, excellent; 2, good; 3, use results with care. Selected means a 10 km subset was selected and produced by RMGSC personnel. Used means used for pond statistics.

Table 3. The Number of Images Analyzed and Their Quality

Quality Site	1999				2000				2001				Grand Totals
	1	2	3	Total Used/Selected	1	2	3	Total Used/Selected	1	2	3	Total Used/Selected	
Beaupo		5	1	6/17	1	10	2	14/63	0	11	0	11/50	30/130
Cacana		1	4	5/22	1	8	1	11/43	0	4	4	8/36	23/101
Cafram		3	5	7/18	1	4	3	8/29	3	9	3	15/72	31/119
Esiber				None acquired	3	5	1	9/65	1	4	3	8/40	17/105
Total for Year	0	9	10	18/57 (out of 160 acquired)	6	27	7	42/200 (out of 511 acquired)	4	28	10	42/198 (out of 385 acquired)	101/455 (out of 1056 acquired)

Each processed image has associated data products. Data products are of two types: image files and data files. Table 4 provides a summary of all data products.

2.1.1 Image Files

1. Browse images in PNG format show the grid of 500 m square cells over the surface type map. The rows and columns on the browse images can be used to locate particular cells, by row, in the data spreadsheets. These are low-resolution images used for reference, not for analysis. Figures 3a-d and 4a-c give examples of browse images. For images where clouds or artifacts have been masked, both unmasked and masked browse images are available. The browse images range in size from about 20 KB to about 150 KB each. To view the browse images, you may use the [Browse Image Spreadsheet Tool \(BIST\)](#).
2. GeoTIFF binary images are 10,000 x 10,000 1 m pixels, about 96 MB per image (Some images were written in compressed format when the files were created. These are smaller.) Image files for two-class images have values indicating missing, water, or ice. Those for three-class images have values indicating missing, open water, melt pond, or ice. For images where clouds or artifacts have been masked, both unmasked and masked GeoTIFF images are available. Figures 5a and 5b gives an indication of the coverage and the resolution of these files. Figure 6 is a screen shot showing the masked and unmasked version of the TIFF images of three scenes.

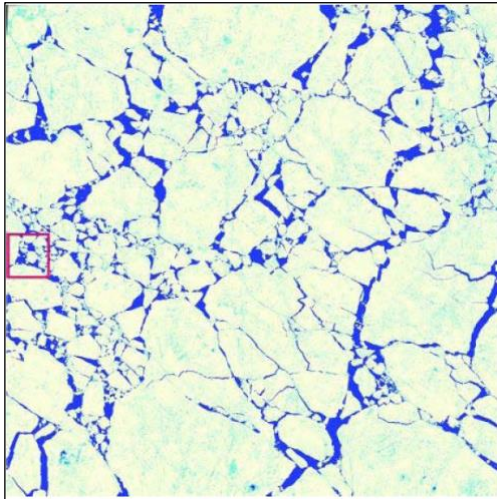


Figure 5a. A GeoTIFF file covering 10km by 10 km at 1 m resolution.

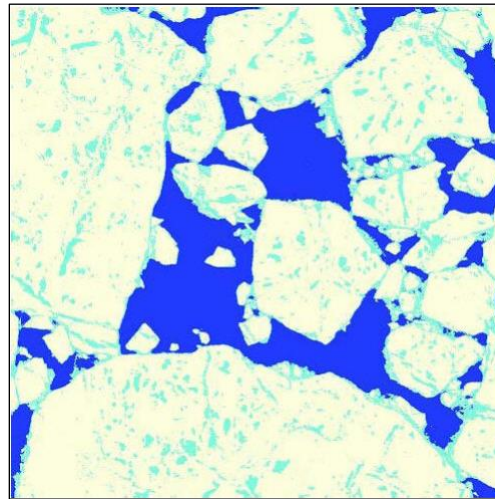


Figure 5b. A zoomed view of the surface map within the red square in Figure 5a.

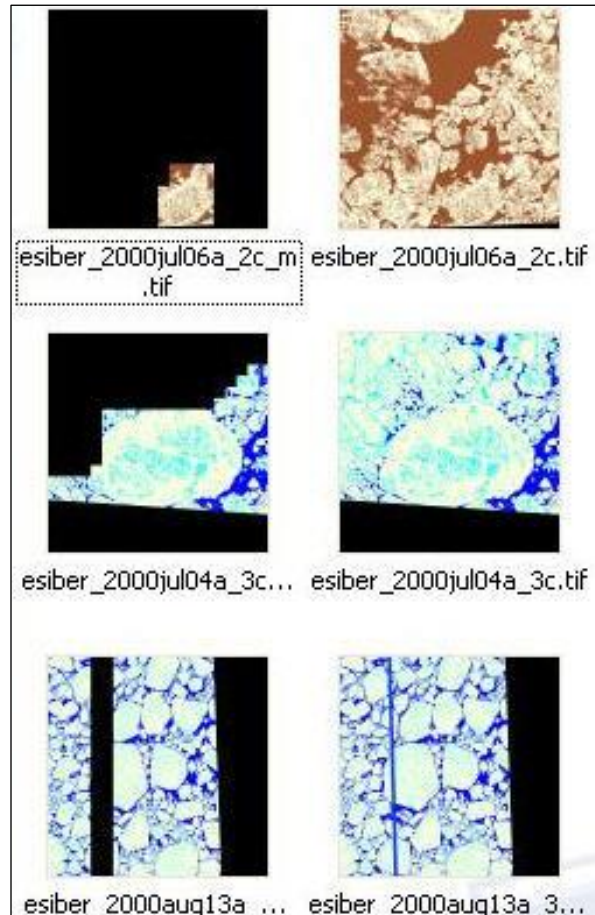


Figure 6. Masked (left) and unmasked (right) versions of GeoTIFF images. Both versions are included in the data set. Unmasked image files usually have some missing data before processing, as shown by the black areas in the images on the right.

2.1.2 Data Files for Surface Type Coverage Statistics

For each site and year, there is one Microsoft Excel file (workbook) containing a worksheet for each processed image that has the composition of each cell, in fraction covered by pond, open water, and ice. There is also an ASCII text file for each image with the same information as in the Excel file. Missing values are indicated by a value of 9.99. Figure 7 is an example of an ASCII file and worksheet.

	A	B	C	D	E	F	G	H	I	J	K	L	M
1	cell	ice	pond	water	owtr								
2	101	0.94	0.00	0.06	0.00								
3	102	0.98	0.00	0.02	0.00								
4	103	0.63	0.00	0.37	0.00								
5	104	0.93	0.00	0.07	0.00								
6	105	0.97	0.00	0.03	0.00								
7	106	0.74	0.00	0.26	0.00								
8	107	0.62	0.00	0.38	0.00								
9	108	0.56	0.00	0.44	0.00								
10	109	0.97	0.00	0.03	0.00								
11	110	0.92	0.00	0.08	0.00								
12	111	0.78	0.00	0.22	0.00								
13	112	0.78	0.00	0.22	0.00								
14	113	0.64	0.00	0.36	0.00								
15	114	0.66	0.00	0.34	0.00								
16	115	0.83	0.00	0.17	0.00								
17	116	0.80	0.00	0.20	0.00								
18	117	0.82	0.00	0.18	0.00								
19	118	0.99	0.00	0.01	0.00								
20	119	1.00	0.00	0.00	0.00								
21	120	0.99	0.00	0.01	0.00								
22	201	0.75	0.00	0.25	0.00								
23	202	0.71	0.00	0.29	0.00								
24	203	0.49	0.00	0.51	0.00								
25	204	0.69	0.00	0.31	0.00								
26	205	0.61	0.00	0.39	0.00								
27	206	0.60	0.00	0.40	0.00								
28	207	0.94	0.00	0.06	0.00								
29	208	0.96	0.00	0.04	0.00								
30	209	0.74	0.00	0.26	0.00								
31	210	0.91	0.00	0.09	0.00								
32	211	0.77	0.00	0.23	0.00								
33	212	0.93	0.00	0.07	0.00								
34	213	0.89	0.00	0.11	0.00								
35	214	0.93	0.00	0.07	0.00								
36	215	0.98	0.00	0.02	0.00								
37	216	1.00	0.00	0.00	0.00								
38	217	0.96	0.00	0.04	0.00								
39	218	0.89	0.00	0.11	0.00								
40	219	0.94	0.00	0.06	0.00								
41	220	0.89	0.00	0.11	0.00								
42	301	0.82	0.00	0.18	0.00								
43	302	1.00	0.00	0.00	0.00								
44	303	1.00	0.00	0.00	0.00								
45	304	0.32	0.00	0.68	0.00								
46	305	0.76	0.00	0.24	0.00								
47	306	0.93	0.00	0.07	0.00								
48	307	0.61	0.00	0.39	0.00								
49	308	0.82	0.00	0.18	0.00								
50	309	0.76	0.00	0.24	0.00								
51	310	0.63	0.00	0.37	0.00								
52	311	0.88	0.00	0.12	0.00								
53	312	0.97	0.00	0.03	0.00								
54	313	0.81	0.00	0.19	0.00								
55	314	0.91	0.00	0.09	0.00								
56	315	1.00	0.00	0.00	0.00								
57	316	0.97	0.00	0.03	0.00								

Figure 7. Example of a surface type coverage statistics spreadsheet, with coverage in hundredths of percent. There is a worksheet for each image processed. Each worksheet has a row for each 500 m square cell. For example, 101 refers to row 1, column 1 in the grid (refer to the corresponding PNG browse files). Water is the sum of pond and open water.

2.1.3 Data Files for Pond Size Statistics

For each site and year, there is one Excel file containing a worksheet for each processed image with summary pond size and surface type coverage statistics for each selected cell (usually two to six cells were selected from each image). In addition, there is a worksheet with pond size statistics as well as sizes for each pond, so that frequency distributions of pond size can be made. These worksheets are illustrated in Figures 8 and 9. Figure 10 is an example of a pond size frequency distribution created from the statistics file. Missing is indicated by a value of 9.99. The smallest pond that can be resolved is 1 m.

Note: Images for which only two classes, ice and water, could be distinguish may still have pond size statistics. If there are pond size statistics for a 2c image, they were arrived at by choosing the cells for the pond size statistics by eye so that they are entirely on a floe. Done this way, any water would be pond, not lead water. If applicable, one may view both the masked and unmasked PNG browse file to see, based on row and column, what cells were chosen.

1	Image Name	Cell Reference (row-column)	Number of Ponds	Mean Pond Size (sq m)	Minimum Pond Size (sq m)	Maximum Pond Size (sq m)	Surface Class Fraction (%)		
							Pond	Ice or Snow	Open Water
2									
3	esiber_2000aug27a_3c	03-07	1158	26.31	1	989	12	88	0
4	esiber_2000aug27a_3c	04-07	1154	30.08	1	3,128	14	86	0
5	esiber_2000aug27a_3c	09-10	794	28.08	1	2,980	9	89	2
6	esiber_2000aug27a_3c	09-11	1027	37.83	1	12,362	15	85	0
7	esiber_2000aug27a_3c	10-10	833	24.70	1	2,649	8	86	6
8	esiber_2000aug27a_3c	10-11	1035	51.23	1	6,442	21	69	10
9	esiber_2000aug27a_3c	12-13	1202	30.79	1	3,796	15	70	13
10	esiber_2000aug27a_3c	12-14	1152	29.19	1	1,891	13	65	22
11	esiber_2000aug27a_3c	13-12	1091	37.71	1	3,067	16	76	8
12	esiber_2000aug27a_3c	13-14	1227	40.10	1	5,536	20	80	0
13									

Figure 8. Illustration of a summary worksheet for pond size statistics. There is a row for each 500 m square cell chosen for pond size analysis.

	A	B	C	D	E	F	G	H	I	J	K	L
1	Site/Date:	esiber_2000aug27a_3c										
2	Row*Column	03-07	04-07	09-10	09-11	10-10	10-11	12-13	12-14	13-12	13-14	
3	Count (Histo >= 1)	1158	1154	794	1027	833	1035	1202	1152	1091	1227	
4	Total Count	30464	34718	22298	38852	20579	53024	37006	33630	41138	49204	
5	Min Pond Size	1	1	1	1	1	1	1	1	1	1	
6	Max Pond Size	989	3128	2980	12362	2649	6442	3796	1891	3067	5536	
7	Mean Pond Size	26.307427	30.084922	28.083123	37.830574	24.704682	51.230918	30.787022	29.192708	37.706691	40.101059	
8	Stddev	78.999817	117.95516	144.32339	401.58145	130.38155	321.0278	174.29371	119.00293	157.10121	197.56685	
9	pond stats:	989	3128	2980	12362	2649	6442	3796	1891	3067	5536	
10		929	958	1744	2372	1655	5256	2896	1812	1481	1498	
11		862	861	1301	1185	1277	2672	1842	1267	1445	1479	
12		809	816	853	1016	841	2552	1289	951	1287	1292	
13		742	701	847	1014	587	2505	1081	908	1149	1119	
14		559	631	491	966	573	2326	1028	849	988	1111	
15		435	583	479	929	561	1871	889	755	912	920	
16		433	510	450	723	533	1864	812	681	899	848	
17		388	492	433	660	453	1246	791	664	879	726	
18		375	448	420	462	389	976	753	604	865	712	
19		365	443	352	373	310	639	746	514	850	616	
20		361	438	346	363	288	586	696	513	805	604	
21		357	403	332	345	219	565	576	497	785	569	
22		319	391	209	338	210	530	563	482	666	537	
23		310	270	198	311	207	521	557	476	618	537	
24		304	263	183	296	189	483	499	471	617	537	
25		291	263	181	278	189	483	490	461	598	505	
26		290	254	170	251	183	457	438	431	530	499	
27		284	248	164	249	180	430	416	427	526	490	
28		275	242	130	243	176	417	394	407	517	472	
29		273	233	127	233	165	407	342	349	442	470	
30		270	230	125	220	135	392	312	345	437	442	
31		265	230	115	210	133	374	308	344	427	425	

Figure 9. Illustration of a worksheet showing individual pond sizes in square meters for the same cells as in Figure 8.

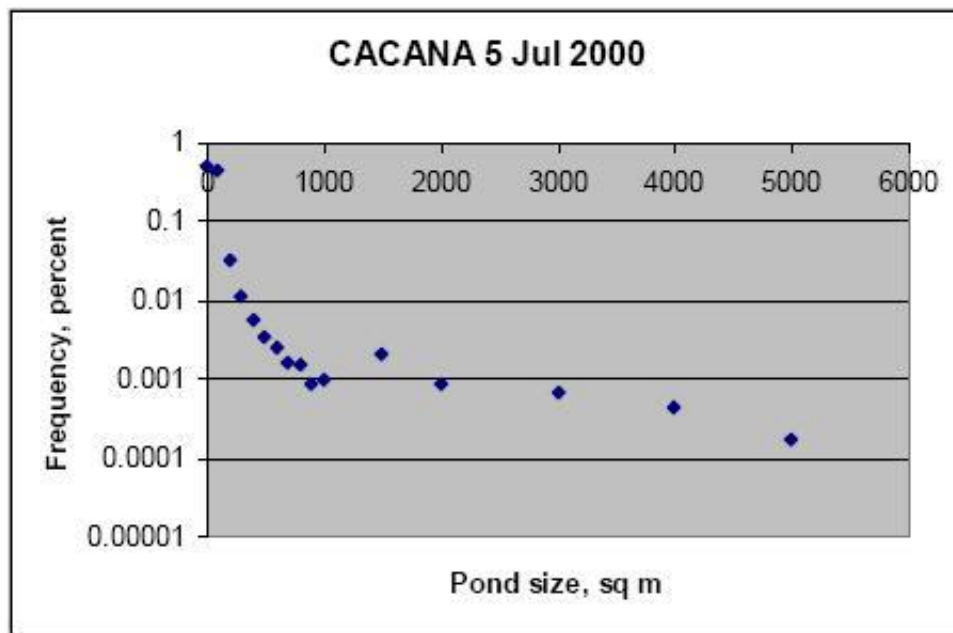


Figure 10. A frequency distribution plot created from pond size statistics.

2.1.4 Data File Summary Information

There is no Cafram_2002_pondsize_stats file available. There are no Cacana 2002 pond size data available, and some summary statistics are missing from Cacana_2001_pondsize_stats. The

workbook image_file_summary.xls is the ancillary data directory; it notes other missing products and has information on product quality.

Table 4. Summary of Data Products

Description	File Format	Example File Name ¹	Naming Convention	Parent Directory	Size	Total # of Files	Example Figures
Surface type map browse images, unmasked	PNG	beafo_1999sep14a_2c.png	Site, year, month, day, <i>a</i> for first in a possible series, <i>2c</i> for a two surface class image, or <i>3c</i> for a 3 class image	G02159_PNGs/1999_png	About 20KB to 150KB	106	See Figure 3
Surface type map browse images, masked	PNG	beafo_1999sep14a_2c_mask.png	Site, year, month, day, <i>a</i> for first in a possible series, <i>2c</i> for a two surface class image, <i>mask</i> to indicate that cloudy or otherwise bad cells have been masked.	G02159_PNGs/1999_png	About 20KB to 150KB	59	See data directory
Surface type maps at 1 m resolution, unmasked	GeoTIFF binary	esiber_2000aug13a_3c.tif	Site, year, month, day, <i>a</i> for first in a possible series, <i>3c</i> for a three surface class image (two class images have <i>2c</i>)	G02159_GeoTIFFs	96MB	116	See Figures 5 and 6
Surface type maps at 1 m resolution, masked	GeoTIFF binary	esiber_2000aug13a_3c_m.tif	Site, year, month, day, <i>a</i> for first in a possible series, <i>3c</i> for a three surface class image, <i>m</i> to indicate that cloudy or otherwise bad cells have been masked.	G02159_GeoTIFFs	96MB	60	See Figure 6

Description	File Format	Example File Name ¹	Naming Convention	Parent Directory	Size	Total # of Files	Example Figures
Composition of each image cell, in fraction covered by pond, open water, and ice	Excel spreadsheets	beaufo_1999_irt_stats.xls {beaufo_1999jul28a_3c_stats_v1.0}	Site, year, irt_stats for cell surface class coverage percentages by cell, output from the IRT software operating on masked TIFF images (site, year, month, day, <i>a</i> for first in a possible series, <i>3c</i> for a three surface class image, <i>stats</i> for surface coverage percentages)	G02159_Pond_statistics_spreadsheets	62KB – 2.2 MB	10	See Figure 7
Pond size and surface type coverage statistics for selected cells (usually two to six cells were selected from each image).	Excel spreadsheets	beaufo_1999_pondsize_stats.xls {jul28a_3c_ponds_v1.0} beaufo_1999_stats.xls {jul28a_3c_summary_v1.0}	Site, year, stats for coverage and pond size statistics (month, day, <i>a</i> for first in a possible series, <i>3c</i> for a three surface class image, <i>ponds</i> for pond size statistics and numbers.) As above, with <i>_sum</i> indicating summary information on pond size and class coverage for the selected cells.	G02159_Pond_statistics_spreadsheets	62KB – 2.2 MB	10	See Figures 8 and 9

Description	File Format	Example File Name ¹	Naming Convention	Parent Directory	Size	Total # of Files	Example Figures
Surface coverage statistics for each cell. (the output of the IRT software, and the same information as in Excel worksheets like beaufo_1999_stats.xls) (jul28a_3c_sum)	ASCII Text	cacana_1999aug16a_3c_stats_v1.0.txt	Site, year, month, day, <i>a</i> for first in a possible series, <i>3c</i> for a three surface class image, <i>stats</i> for surface coverage percentages.	G02159_Cell_coverages_txt_files	12KB	117	See data directory
As above, but for images that required masking of bad cells.	ASCII Text	cacana_1999aug16a_3c_stats_m_v1.1.txt	Site, year, month, day, <i>a</i> for first in a possible series, <i>3c</i> for a three surface class image, <i>stats</i> for surface coverage percentages, <i>m</i> to indicate that cloudy or otherwise bad cells have been masked.	G02159_Cell_coverages_txt_files	12KB	60	See data directory
Images showing the site locations on a map of sea ice extent from the Sea Ice Index by month and year	JPG image files	SeaIceIndex_May_2001_SiteMap.jpg	Ice extent image from the Sea Ice Index (http://nsidc.org/data/seaice_index), month, year.	G02159_Ancillary	16KB	15	See Figure 2
A Google Earth file with site locations.	KML	RMGSC_Ice_Sites_g02159.kml		G02159_Ancillary			See data directory

Description	File Format	Example File Name ¹	Naming Convention	Parent Directory	Size	Total # of Files	Example Figures
List of all images processed with information about each image.	Excel spreadsheet	Image_file_summary.xls		G02159_Ancillary			See data directory

¹An exemplified worksheet name, if applicable, is enclosed in brackets {}.

3 DATA ACQUISITION AND PROCESSING

3.1 Summary

High-resolution visible band imagery was acquired over the four sites (three in 1999) during the summers of 1999, 2000, 2001. Refer to Figure 1. Because of cloud cover, many more images were acquired than were used for analysis. A first pass of the imagery was made to eliminate clearly unusable imagery. Then 10 km square subsets were cut out from the remaining images. As shown in Table 1, a total of 1056 images were acquired by ASC and sent to RMGSC for the project. Of these, 455 were selected as potentially usable, and 101 were used for pond statistics.

Surface type maps were produced by supervised maximum likelihood classification using hand selected training sets. Notes on the quality of each image, and the state of the ice cover, were made in an Excel spreadsheet. For images deemed suitable for classification, training sets were chosen, and notes were made on the quality of the surface type map produced. Not all images were of good enough quality (with sufficient dynamic range, and cloud-free areas) to allow classification into three surface types (pond, open water, and ice). The others were classified into two surface types: water and ice. The one-meter resolution surface type map images were then used as input to a routine (the Ice Reconnaissance Toolbox) that produced output files with the percentage coverage of each type in each cell. These files were kept as ASCII files, and also included as worksheets in Excel files.

Clouds, of course, often obscured the surface, but when clouds were present in cloud streets, or in patches, it was possible to select the 500m cells that were cloudy using an area of interest (AOI) function in ERDAS Imagine, and create a cloud masked GeoTIFF surface classification map for pond coverage statistics. In some images only a few cells were usable, but these were included when they were needed to make the time series more complete than it would be otherwise. The

same masking procedure was used to mask an artifact that appeared in many images. Almost half of the images from which statistics were derived required masking.

Pond size statistics were produced by carefully selecting a few cells from each usable image and using ERDAS Imagine functions that isolated each pond as an individual object. The size (in square meters) of each pond within the cell was then extracted, and summary statistics for the cell compiled.

3.2 Data Processing

Imagery was analyzed using the following procedure.

Step 1. A subset of imagery from the summers of 1999, 2000, and 2001 was selected for analysis based on cloud conditions and retrieved from an online database. A 10 km by 10 km grid, with 500 m cell size, was fitted over the image, placing it to avoid cloudy areas as much as possible. The 10 km by 10 km area was used for the surface type map.

Step 2. The surface type map was created using maximum likelihood classification to segment images. Classification and extraction of pond size statistics was done using ERDAS Imagine software tools. Manual selection of image intensity training sets for each surface type in each image was required. The number of surface types that can be distinguished based on image pixel intensity varies from image to image. It was usually possible to distinguish either two classes: non-water (snow or ice), and water (melt pond or open water); or three (melt pond, open water, and ice).

Errors in classification can result from class distribution overlap, the subjectivity involved in picking training sets, and from sub-resolution melt ponds. If class pixel intensity distributions are well separated, the error resulting from class overlap is low. The separation of intensity distributions for different surface types depends on the albedo of those types and on the illumination conditions, as well as the dynamic range of the instrument or film that records the scene. ERDAS Imagine software tools were used to evaluate class separation (and therefore how many surface types can reliably be identified in an image) and monitor how well the selected training areas represented the classes. Usually, 5 to 10 training areas were used to define an intensity distribution for each class (open water required only one).

The resolution of the imagery is about 1 meter. Therefore, melt ponds smaller in size than one meter will not be resolved. Fetterer and Untersteiner 1998a address the accuracy of melt pond statistics derived from reconnaissance imagery.

Step 3. Cells contaminated by cloud cover were identified by manual inspection of the original imagery, using standard image processing tools to stretch the images for better cloud detection. Cloudy cells were masked out in the version of the surface type map used to derive pond coverage statistics. In images where open water is indistinguishable from pond water on the basis of pixel intensity, cells that have open water in them were identified so that these areas of open water are not included in melt pond size or coverage statistics. Open water was identified using shape of features.

Step 4. ERDAS Imagine software was used to create output files of pond size statistics. There are relatively few of these, because process was time consuming and could not be automated.

Step 5. The Ice Reconnaissance Toolbox (IRT) was used to read the one-meter resolution surface type map GeoTIFF images and create surface type coverage statistics text files with the percentage coverage of each type in each 500m square cell. The IRT package consists of Perl script that calls an IDL procedure, an HTML document Users Guide, test script, and test data.

Step 6. Coverage statistics were compiled in Excel files.

Step 7. PNG browse images were made using ArcGIS.

After image processing was complete, it was discovered that due to misregistration, the IRT Toolbox software omitted as "masked" certain good cells. These were inserted in the ASCII text file, using the results from processing the unmasked files. These files have v1.1 in the file name.

3.3 Quality Assessment

Sun angle and light levels varied, and images varied in dynamic range. This necessitated using supervised maximum likelihood classification for the best possible classification result. Usually, several iterations with slightly different signature files were performed before the final product was chosen. The classified and original image were flickered on the screen to gauge the best result. An unsupervised method, isodata (Duda and Hart 1973), gave inconsistent results, working well on some images and not at all on others.

Producing the surface type maps was a subjective process for which no independent checks were available. Limitations include the 1 m resolution of the images (smaller ponds are not detected), and false detections because of ridge shadows (usually classified as pond), thin ice in leads (sometimes classed as pond) or shelves of submerged ice around floes (sometimes classified as ponds). Based on multiple classification of the same images, we estimate the accuracy of the pond coverage at ± 7 percent for quality 2 and better images. Some results of classification on the same base image vary much more, but in these cases the difference is intentional. See, for example, the

results for cafram1999aug23a and 23b, and the notes on these results in image_file_summary.xls. This data set cannot approach the accuracy of detailed surface observations like those acquired at SHEBA, but it does provide spatial coverage and a large number of samples that would be difficult to acquire in any other way.

The Excel file, Image_file_summary.xls, has a quality ranking for each image. These were assigned subjectively when the supervised classification was performed, and indicate confidence in the pond coverage statistics. Quality is ranked optimal (highest confidence in results), good, questionable (use results with care) and poor. Those ranked poor will not have surface type coverage statistics data, but may have been processed only to obtain image files that show floe morphology.

In the three class data files, ice plus open water plus pond may not sum exactly to 1 (100 percent). Pond plus open water may not exactly equal the water value. Summed amounts may be off by 1 percent. However, ice plus water will equal 1.

If the amount of ice present in a cell is less than 1 percent, the data may show 0 percent. For example, see the browse file for beaufor_2000aug15a_2c. The data for row 12, column 19 has 1 percent ice. The data for row 12, column 20 has 0 percent ice, even though a very small amount of ice is evident for this cell in the browse image.

Before using statistics files, examine both the corresponding browse image, the notes and quality ranking, and the summary information file, so that limitations in the classification accuracy for each particular image are understood.

4 REFERENCES AND RELATED PUBLICATIONS

Barber D. G., J. Yackel . The physical, radiative and microwave scattering characteristics of melt ponds on Arctic landfast sea ice. *International Journal of Remote Sensing*, Volume 20, Number 10, 10 July 1999 , pp. 2069-2090(22)

Duda, Richard O., and Peter E. Hart. 1973. *Pattern classification and scene analysis*. John Wiley and Sons, Inc. 482 pp.

Eicken, H., H. R. Krouse, D. Kadko, and D. K. Perovich (2002), Tracer studies of pathways and rates of meltwater transport through Arctic summer sea ice, *J. Geophys. Res.*, 107(C10), 8046, doi:10.1029/2000JC000583.

Fetterer, F., and N. Untersteiner. 1998a. Observations of Melt Ponds on Arctic Sea Ice. *Journal of Geophysical Research*, 103 (C11), 24,821-24,835

- Fetterer, F., and N. Untersteiner, Melt pond coverage statistics from classified satellite data, in International Geoscience and Remote Sensing Symposium, (on CD-ROM), IEEE 97CH36174, Seattle, WA, 1998b.
- Grenfell, T.C., and G.A. Maykut. The optical properties of ice and snow in the Arctic basin. *Journal of Glaciology*, 18 (80), 445-463, 1977.
- Kwok, R. 2014. Declassified high-resolution visible imagery for Arctic sea ice investigations: an overview. *Remote Sensing of the Environment* 142: 44-56. doi: 10.1016/j.rse.2013.11.015.
- Langleben, M.P. Albedo of melting sea ice in the southern Beaufort sea, *Journal of Glaciology*, 10 (58), 101-104, 1971.
- Moritz, R.E., J.A. Curry, A.S. Thorndike, and N. Untersteiner, SHEBA: a Research Program on the Surface Heat Budget of the Arctic Ocean, 34 pp., Polar Science Center, Applied Physics Laboratory, University of Washington, Seattle, 1993.
- Morassutti, M.P., and E.F. LeDrew, Albedo and Depth of Melt Ponds on Sea Ice, *International Journal of Climatology*, 16, 817-838, 1996
- NSIDC. 2000. SHEBA Reconnaissance Imagery, Version 1.0. Boulder, Colorado USA: National Snow and Ice Data Center. Digital media.
- Perovich, D.K., and W.B. Tucker III, Arctic sea-ice conditions and the distribution of solar radiation during summer, *Annals of Glaciology*, 25, 445-450, 1997.
- Perovich, D.K., C.S. Roesler, and W.S. Pegau, Variability in Arctic sea ice optical properties, *Journal of Geophysical Research*, 103 (C1), 1193-1208, 1998.
- Perovich, D. K., T. C. Grenfell, J. A. Richter-Menge, B. Light, W. B. Tucker III, and H. Eicken, Thin and thinner: Sea ice mass balance measurements during SHEBA, *J. Geophys. Res.*, 108(C3), 8050, doi:10.1029/2001JC001079, 2003.
- Perovich, D.K., et al., Year on ice gives climate insights, *EOS, Transactions of the American Geophysical Union*, 80, 481, 485-486, 1999.
- Perovich, D.K., T.C. Grenfell, B. Light, J.A. Richter-Menge, M. Sturm, W.B. Tucker III, H. Eicken, G.A. Maykut, and B. Elder, SHEBA: Snow and Ice Studies, CD-ROM, October, 1999.
- Perovich, D. K., W. B. Tucker III, and K. A. Ligett (2002), Aerial observations of the evolution of ice surface conditions during summer, *J. Geophys. Res.*, 107(C10), 8048, doi:10.1029/2000JC000449
- Richelson, J.T., Scientists in black, *Scientific American*, 278 (2), 48-55, 1998.
- Tschudi, M. A., J. A. Curry, and J. A. Maslanik (2001), Airborne observations of summertime surface features and their effect on surface albedo during FIRE/SHEBA, *J. Geophys. Res.*, 106(D14), 15,335-15,344.

Tschudi, M.A., J.A. Curry, and J.A. Maslanik, Determination of areal surface-feature coverage in the Beaufort Sea using aircraft video data, *Annals of Glaciology*, 25, 434-438, 1997.

Yackel, J. J.; Barber, D. G.; Papakyriakou, T. N.; Breneman, C., First-year sea ice spring melt transitions in the Canadian Arctic Archipelago from time-series synthetic aperture radar data, 1992-2002, *Hydrological Processes*, vol. 21, Issue 2, pp.253-265

4.1 Related Data Collections

[SHEBA Reconnaissance Imagery](#)

[Sea Ice Melt Pond Data from the Canadian Arctic](#)

4.2 Related Websites

[The Global Fiducials Library](#)

SHEBA Snow and Ice Studies, Version 1.0, October 11, 1999 (Obtainable from D. Perovich, CRREL, 72 Lyme Road, Hanover, NH, USA 03755.)

5 CONTACTS AND ACKNOWLEDGMENTS

Florence Fetterer
National Snow and Ice Data Center
University of Colorado Boulder
CIRES
449 UCB
Colorado 80309-0449 USA

Stanley Wilds
Jeffrey Sloan
Rocky Mountain Geographic Science Center
Denver Federal Center
Lakewood, CO USA

Acknowledgements:

The National Science Foundation (NSF Award ID 0105057) and the USGS Rocky Mountain Geographic Science Center (RMGSC) supported development of this data set. Support for distribution of the data is being provided by the NOAA National Geophysical Data Center. Stan Wilds provided engineering and technical support with all aspects of processing, including the RMGSC Image Library and ERDAS Imagine. Laurie Temple led work on image acquisition and metadata, and handled requests to the intelligence community for release of data as Image Derived Products. NSIDC scientific programmer Terry Haran developed the Ice Reconnaissance Toolbox software. Former NSIDC scientific programmer Christopher Haggerty collaborated in producing these data. We also acknowledge support from Jeff Sloan and Earl Wilson, RMGSC

Geographic Technology and Applications Team, and Michael Hutt, Associate Chief, RMGSC. The KML file was provided by Jeff Sloan.

Distribution of the data set from NSIDC is supported by funding from NOAA's National Environmental Satellite, Data, and Information Service (NESDIS) and the National Geophysical Data Center (NGDC).

6 DOCUMENT INFORMATION

6.1 Document Authors

Florence Fetterer authored this document. Deann Miller prepared this document.

6.2 Publication Date

August 2008

6.3 Date Last Updated

February 2011, A. Windnagel: Added note to Section 3 under Data Files for Pond Size Statistics.

October 2009, A. Windnagel: Added a data set to the Other Related Data Collections section.